

(presumably constant at about  $150 \text{ km s}^{-1}$ ). Combined with the presence of SiO masers in W43A<sup>14</sup>, which are detected in very few proto-planetary nebulae<sup>9</sup>, and with the OH masers such as those typically found in OH/infrared stars (Fig. 2), this estimate strongly suggests that we are observing a star in transition. It is likely that the “molecular jet” traced by H<sub>2</sub>O masers was created in the OH/infrared star phase, before the transition to a proto-planetary nebula. Comparing the above timescales with the duration of significant mass-loss rate (1,000–4,000 years)<sup>28</sup> from an OH/infrared star (see also Fig. 2), a molecular jet should affect the development of nebula morphology from the beginning of its formation<sup>1</sup>. However, the driving object and the formation mechanism of the jet are still unclear. W43A could be an AGB star able to create a collimated jet driven by the magnetic force owing to the dynamo action at the interface between the rapidly rotating core and the more slowly rotating envelope of the star<sup>6</sup>. Alternatively, W43A could be a binary system where the ejected material from a mass-losing star falls onto an accretion disk surrounding a companion that creates the jet<sup>29,30</sup>. □

Received 19 October 2001; accepted 2 April 2002; doi:10.1038/nature00788.

1. Sahai, R. & Trauger, J. T. Multipolar bubbles and jets in low-excitation planetary nebulae: toward a new understanding of the formation and shaping of planetary nebulae. *Astron. J.* **116**, 1357–1366 (1998).
2. Sahai, R., te Lintel Hekkert, P., Morris, M., Zijlstra, A. & Likkell, L. The “Water-Fountain Nebula” IRAS 16342 – 3814: Hubble Space Telescope/Very Large Array study of a bipolar protoplanetary nebula. *Astrophys. J.* **514**, L115–L119 (1999).
3. Alcolea, J., Bujarrabal, V., Sanchez, C. C., Neri, R. & Zweigle, J. The highly collimated bipolar outflow of OH 231.8 + 4.2. *Astron. Astrophys.* **373**, 932–949 (2001).
4. Zijlstra, A. A. *et al.* Bipolar outflows in OH/IR stars. *Mon. Not. R. Astron. Soc.* **322**, 280–308 (2001).
5. Miranda, L. F., Gómez, Y., Anglada, G. & Torrelles, J. M. Water-maser emission from a planetary nebula with a magnetized torus. *Nature* **414**, 284–286 (2001).
6. Blackman, E. G., Frank, A., Markiel, J. A., Thomas, J. H. & Van Horn, H. M. Dynamos in asymptotic-giant-branch stars as the origin of magnetic fields shaping planetary nebulae. *Nature* **409**, 485–487 (2001).
7. Diamond, P. J., Norris, R. P., Rowland, P. R., Booth, R. S. & Nyman, L.-A. The circumstellar envelopes around OH/IR stars. *Mon. Not. R. Astron. Soc.* **212**, 1–21 (1985).
8. Herman, J. & Habing, H. J. Time variations and shell sizes of OH masers in late-type stars. *Astron. Astrophys.* **59**, 523–555 (1985).
9. Nyman, L.-A., Hall, P. J. & Olofsson, H. SiO masers in OH/IR stars, proto-planetary and planetary nebulae. *Astron. Astrophys. Suppl. Ser.* **127**, 185–200 (1998).
10. van der Veen, W. E. C. J. & Habing, H. J. The IRAS two-colour diagram as a tool for studying late stages of stellar evolution. *Astron. Astrophys.* **194**, 125–134 (1988).
11. Genzel, R. & Downes, D. H<sub>2</sub>O in the Galaxy: sites of newly formed OB stars. *Astron. Astrophys. Suppl. Ser.* **30**, 145–168 (1977).
12. Diamond, P. J. & Nyman, L.-A. in *VLBI and its Impact on Astrophysics* (eds Moran, J. M. & Reid, M. J.) 249–250 (Astronomical Society of the Pacific, San Francisco, 1988).
13. Likkell, L., Morris, M. & Maddalena, R. J. Evolved stars with high velocity H<sub>2</sub>O maser features: bipolar outflows with velocity symmetry. *Astron. Astrophys.* **256**, 581–594 (1992).
14. Nakashima, J. *Observational Study of O-rich Evolved Stars in the Galaxy*. PhD thesis, Graduate Univ. Advanced Studies (2002).
15. Elitzur, M. *Astronomical Masers* (Kluwer Academic, Dordrecht, 1992).
16. Cooke, B. & Elitzur, M. Water masers in late-type stars. *Astrophys. J.* **295**, 175–182 (1985).
17. Chapman, J. M. & Cohen, R. J. MERLIN observations of the circumstellar envelope of VX Sagittarius. *Mon. Not. R. Astron. Soc.* **220**, 513–528 (1986).
18. Lane, A. P. *et al.* H<sub>2</sub>O masers in circumstellar envelopes. *Astrophys. J.* **323**, 756–765 (1987).
19. Bachiller, R. Bipolar molecular outflows from young stars and protostars. *Annu. Rev. Astron. Astrophys.* **34**, 111–154 (1996).
20. Chandler, F. & Guillaudeau, S. The jet-driven molecular outflow of HH 211. *Astron. Astrophys.* **343**, 571–584 (1999).
21. Bloemhof, E. E. Kinematics of the H<sub>2</sub>O masers in W49N: Analysis of the velocity variance-covariance matrix. *Astrophys. J.* **533**, 893–896 (2000).
22. Zinnecker, H., McCaughrean, M. J. & Rayner, J. T. A symmetrically pulsed jet of gas from an invisible protostar in Orion. *Nature* **394**, 862–865 (1998).
23. Elitzur, M., Hollenbach, D. J. & McKee, C. F. Planar H<sub>2</sub>O masers in star-forming regions. *Astrophys. J.* **394**, 221–227 (1992).
24. Furuya, R. S. *et al.* A microjet: a protostar’s cry at birth. *Astrophys. J.* **542**, L135–L138 (2000).
25. Torrelles, J. M. *et al.* Spherical episodic ejection of material from a young star. *Nature* **411**, 277–280 (2001).
26. Marvel, K. B. The circumstellar environment of evolved stars as revealed by studies of circumstellar water masers. *Publ. Astron. Soc. Pacif.* **109**, 1286–1287 (1997).
27. Uchida, Y. & Shibata, K. Magnetodynamical acceleration of CO and optical bipolar flows from the region of star formation. *Publ. Astron. Soc. Jpn* **37**, 515–535 (1985).
28. Lewis, B. M. On the transience of high-latitude OH/IR stars. II. Thermal pulse link. *Astrophys. J.* **560**, 400–412 (2001).
29. Morris, M. Mechanisms for mass loss from cool stars. *Publ. Astron. Soc. Pacif.* **99**, 1115–1122 (1987).
30. Howard, B. E. in *Asymmetrical Planetary Nebulae II: From Origins to Microstructures*, ASP Conference Series (eds Kastner, H., Soker, N. & Rappaport, S.) Vol. 199 115–123 (Astronomical Society of the Pacific, San Francisco, 2000).

**Acknowledgements**

We thank J. Nakashima and S. Deguchi for providing the information concerning SiO maser emission and infrared images of W43A. NRAO is a facility of the National Science Foundation, operated under cooperative agreement by Associated Universities, Inc. H. I. was financially supported by the Research Fellowship of the Japan Society of the Promotion of Science for Young Scientist.

**Competing interests statement**

The authors declare that they have no competing financial interests.

Correspondence and requests for materials should be addressed to H.I. (e-mail: imai@jive.nl).

.....  
**Hidden orbital order in the heavy fermion metal URu<sub>2</sub>Si<sub>2</sub>**

**P. Chandra\*, P. Coleman†, J. A. Mydosh‡ & V. Tripathi†**

\* *NEC, 4 Independence Way, Princeton, New Jersey 08540, USA*  
 † *Center for Materials Theory, Dept of Physics and Astronomy, Rutgers University, Piscataway, New Jersey 08855, USA*  
 ‡ *Kamerlingh Onnes Laboratory, Leiden University, PO Box 9504, 2300 RA Leiden, The Netherlands*

.....  
**When matter is cooled from high temperatures, collective instabilities develop among its constituent particles that lead to new kinds of order<sup>1</sup>. An anomaly in the specific heat is a classic signature of this phenomenon. Usually the associated order is easily identified, but sometimes its nature remains elusive. The heavy fermion metal URu<sub>2</sub>Si<sub>2</sub> is one such example, where the order responsible for the sharp specific heat anomaly at T<sub>0</sub> = 17 K has remained unidentified despite more than seven-teen years of effort<sup>2</sup>. In URu<sub>2</sub>Si<sub>2</sub>, the coexistence of large electron–electron repulsion and antiferromagnetic fluctuations leads to an almost incompressible heavy electron fluid, where anisotropically paired quasiparticle states are energetically favoured<sup>3</sup>. Here we develop a proposal for the nature of the hidden order in URu<sub>2</sub>Si<sub>2</sub>. We show that incommensurate orbital antiferromagnetism, associated with circulating currents between the uranium ions, can account for the local fields and entropy loss observed at the 17 K transition. We make detailed predictions for the outcome of neutron scattering measurements based on this proposal, so that it can be tested experimentally.**

The intermetallic compound URu<sub>2</sub>Si<sub>2</sub> contains a dense lattice of local moments where quantum fluctuations barely prevent spin ordering; the residual antiferromagnetic couplings between the strongly repulsive electrons are large and can drive new types of collective instabilities<sup>2</sup>. At T<sub>0</sub> = 17.5 K, URu<sub>2</sub>Si<sub>2</sub> undergoes a second-order phase transition characterized by sharp discontinuities in bulk properties, including specific heat<sup>4</sup>, linear<sup>4</sup> and non-linear<sup>5,6</sup> susceptibilities, thermal expansion<sup>7</sup> and resistivity<sup>8</sup>. The accompanying gap in the magnetic excitation spectrum<sup>9</sup> suggests the formation of an itinerant spin density wave at this temperature; however, the size of the observed staggered moment<sup>10</sup> (m<sub>0</sub> = 0.03μ<sub>B</sub>) cannot account for the entropy loss at this transition. The distinction between the primary hidden-order parameter and the secondary magnetic-order parameter is clarified by high-field measurements<sup>11,12</sup> which indicate that the bulk anomalies survive up to an applied field strength of 40 tesla (T), whereas the magnetically ordered moment is destroyed by fields less than half this magnitude (15 T) (ref. 13). Furthermore, the size of

the small ordered moment grows linearly with pressure<sup>14</sup>, while the gap associated with the hidden order is relatively robust over this pressure range<sup>15</sup>.

There have been many theoretical proposals for the primary order parameter in URu<sub>2</sub>Si<sub>2</sub> (ref. 16). Two recent nuclear magnetic resonance (NMR) studies have provided insights with crucial consequences for the nature of the hidden order. It has been widely assumed that the spin antiferromagnetism and the hidden order are coupled and homogeneous. However, a recent NMR study of URu<sub>2</sub>Si<sub>2</sub> under pressure<sup>17</sup> indicates that for  $T < T_0$  there exist distinct antiferromagnetic and paramagnetic regions, implying that the magnetic and the hidden orders are phase-separated. This conclusion, supported by muon spin resonance ( $\mu$ SR) data<sup>18</sup>, implies that the hidden-order phase contains no spin order. The observed growth of the staggered spin moment with applied pressure<sup>14</sup> is then simply a volume-fraction effect which develops separately from the hidden order through a first-order transition<sup>19</sup>. At ambient pressure roughly a tenth or less of the system<sup>17,18</sup> is magnetic, with  $m_{\text{spin}} = 0.3\mu_B$ . The main implication of these measurements for theory is that the magnetic and the hidden-order parameters are independent<sup>19</sup>.

In a parallel study, NMR measurements at ambient pressure<sup>20</sup> on URu<sub>2</sub>Si<sub>2</sub> indicate that at  $T \leq T_0$  the central (non-split) silicon NMR linewidth develops a field-independent, isotropic component whose temperature-dependent magnitude is proportional to that of the hidden-order parameter. These results imply an isotropic field distribution at the silicon sites whose root-mean-square value is proportional to the hidden order ( $\psi$ ):

$$\langle B^\alpha(i)B^\beta(j) \rangle = A^2\psi^2\delta_{\alpha\beta} \quad (1)$$

and is about 10 gauss (G) at  $T = 0$ . This field magnitude is too small to be explained by the observed moment<sup>10</sup> which induces a field  $B_{\text{spin}} = (8/3)\pi Ma^{-3} = 100 \text{ G}$  where  $a$  is the  $U-U$  bond length ( $a = 4 \times 10^{-8} \text{ cm}$ ). Furthermore, this moment is aligned along the  $c$  axis, and thus cannot account for the isotropic nature of the local field distribution detected by NMR. These measurements indicate that as the hidden order develops, an isotropically dis-

tributed static magnetic field develops at each silicon site. This is unambiguous evidence that the hidden-order parameter breaks time-reversal invariance.

Guided by these experiments, we now discuss our proposal for the nature of the hidden-order parameter. The magnetic fields at the silicon nuclei have two possible origins<sup>21</sup>: the conduction electron-spin interaction and the orbital shift that is due to current densities. In URu<sub>2</sub>Si<sub>2</sub>, the electron fluid exhibits a strong Ising anisotropy along the  $c$  axis, as measured by the Knight shift<sup>20</sup>; hence, electron-spin coupling cannot be responsible for the observed isotropic fields. It would thus appear that these local fields are induced by currents that develop inside the crystal as the hidden order develops, and accordingly we attribute the observed isotropic linewidth to the orbital shift.

Here we propose that URu<sub>2</sub>Si<sub>2</sub> becomes an incommensurate orbital antiferromagnet at  $T = T_0$  with charge currents circulating between the uranium ions. Similar states have been studied extensively in the context of the two-dimensional Hubbard model<sup>22–26</sup>, particularly in connection with staggered flux phases<sup>27,28</sup>: more recently, commensurate current-density wave order has been proposed to explain the spin-gap phase in the underdoped copper oxide superconductors<sup>29,30</sup>. The planar tetragonal structure of URu<sub>2</sub>Si<sub>2</sub> lends itself naturally to an anisotropic charge instability of this type. Here we show that incommensurate orbital antiferromagnetic order in URu<sub>2</sub>Si<sub>2</sub> can quantitatively account for the existing specific heat and NMR data for  $T \leq T_0$ . To test this, we make specific predictions for neutron scattering. Calculation of the structure factor requires knowledge of the fields throughout the full volume in real-space. The NMR only yields this information at discrete points, so we need some additional input to proceed. In the orbital antiferromagnet, the spatial dependence of the fields throughout the sample is determined by the requirement that the field distribution at the silicon sites is isotropic. Using this approach, we are able to link quantitatively the fields observed by NMR to the large specific heat anomaly that develops at  $T_0$ . We also use the spatial field distribution associated with the incommensurate orbital antiferromagnet to predict the position, intensity and form-factor associated

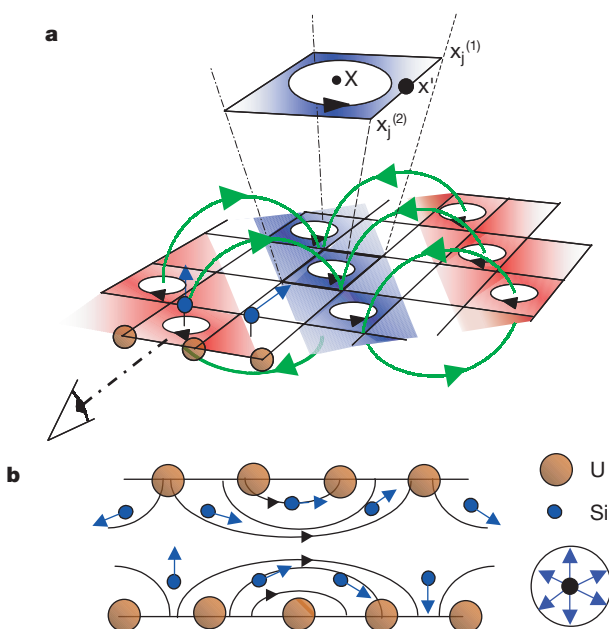


**Figure 1** Magnetic field distribution associated with incommensurate orbital currents in the (0, 0, 1) plane. **a**, Schematic illustration of incommensurate orbital currents, showing resulting magnetic fields above and below the (0, 0, 1) plane.  $X_j^{(1)}$  and  $X_j^{(2)}$  are the

coordinates of the plaquette, and  $X'$  denotes the coordinate along a uranium–uranium bond. **b**, Side view showing how proposed field distribution is isotropic at silicon sites with a staggered current distribution between layers corresponding to  $Q = (0.16, 0.16, 1)$ .

with neutron scattering peaks on a surface of constant anisotropy in momentum space centred on the origin.

We begin by estimating the local fields at the silicon sites that are due to orbital currents circulating around the square uranium plaquettes in the  $a$ - $b$  plane. On dimensional grounds, the current along the  $U$ - $U$  bond is given by  $I \approx e\Delta/\hbar$  where  $\Delta$  is the gap associated with the formation of hidden order. Then the field induced at a height  $a$  above a plaquette is  $B \approx (2/ac)(e\Delta/\hbar) = 11$  G, in good agreement with the local field strength detected in NMR measurements; here<sup>4,9-11</sup> we have used  $\Delta = 110$  K. The resulting orbital moment,  $m_{\text{orb}} \approx 0.02\mu_B$ , is comparable to the effective spin moment at ambient pressure ( $m_0 = m_{\text{spin}} P_{\text{amb}} = 0.10 m_{\text{spin}} = 0.03\mu_B$ ). We emphasize that an orbital moment produces a local field an order of magnitude less than that associated with a spin moment of the same value; the low field strengths observed at the silicon sites are quantitatively consistent with our proposal that they originate from charge currents.

An orbital moment,  $m_{\text{orb}} = 0.02\mu_B$ , can also account for the sizable entropy loss at the transition. In a metal the change in entropy is given by  $\Delta S = \Delta\gamma_n T_0$ , where  $\Delta\gamma_n$  is the change in the linear specific heat coefficient resulting from the gapping of the Fermi surface.  $\Delta\gamma_n$  is inversely proportional to the Fermi energy  $\epsilon_F$  of the gapped Fermi surface. Thus, in general, the change in entropy per unit cell is given by  $\Delta S \approx k_B(k_B T_0/\epsilon_F)$ . Exploiting the mean-field nature of this transition ( $2\Delta \propto T_0$ ), we find that for the orbital antiferromagnet (OAFM):

$$\Delta S_{\text{OAFM}} \approx k_B \left( \frac{m_{\text{orb}}}{\mu_B} \right) = 0.02k_B \left( \frac{\mu_B^*}{\mu_B} \right) \quad (2)$$

where  $\mu_B^* = (e/\hbar c)a^2\epsilon_F$  is the saturated orbital moment reached when the hidden-order gap  $\Delta$  is approximately  $\epsilon_F$ . The ratio  $\mu_B/\mu_B^* = (a_0/a)^2(\epsilon_H/\epsilon_F)$ , where  $a_0$  is the Bohr radius and  $\epsilon_H = e^2/(2a_0)$  is the energy of a hydrogen atom. For URu<sub>2</sub>Si<sub>2</sub>, the very large size of  $(\epsilon_H/\epsilon_F) \approx 10^3$  produced by the large mass renormalization of the heavy electrons actually offsets the small ratio  $a_0/a \approx 10^{-1}$ , so that  $\mu_B/\mu_B^* \approx 10$ , and  $\Delta S_{\text{OAFM}} \approx 0.2k_B = 0.3k_B \ln 2$  is a number in good agreement with experiment<sup>4</sup>. The critical field for suppressing the associated thermodynamic anomalies is distinct from its spin counterpart; the ratio  $H_c^{\text{orb}}/H_c^{\text{spin}} \approx \mu_B/\mu_B^* \approx 10$  is qualitatively consistent with the observed critical field of approximately 40 T associated with the destruction of the hidden order<sup>11-13</sup>. From this simple discussion, we see that the sizable entropy loss associated with the development of the orbital antiferromagnetic state is a direct consequence of the strong renormalization of the electron mass in URu<sub>2</sub>Si<sub>2</sub> ( $m^*/m \propto \epsilon_H/\epsilon_F$ ). The absence of such a large effective mass ( $m^*/m \approx 3$ ) in the copper oxides could explain why analogous thermodynamic anomalies are difficult to observe there.

Next we test whether the proposed orbital antiferromagnetism will yield the observed isotropic local fields. We allow the circulating current around a plaquette (see Fig. 1) centred at site  $X$  to develop a modulated magnetization  $M(\mathbf{X}) = \psi e^{i\mathbf{Q}\cdot\mathbf{X}}$ . The current along a bond is then the difference of the circulating currents along its adjacent plaquettes. The field at a silicon site can be computed using Ampere's law, where the relevant vector potential is:

$$\mathbf{A}(\mathbf{x}) = \frac{1}{c} \sum_j \int_{\mathbf{x}_j^{(1)}}^{\mathbf{x}_j^{(2)}} dx' \frac{\mathbf{I}(\mathbf{x}_j)}{|\mathbf{x} - (\mathbf{x}_j + \mathbf{x}')|} \quad (3)$$

where  $\mathbf{x}_j^{(1,2)}$  are the endpoints of the bond at site  $\mathbf{x}_j$ .

The silicon atoms in URu<sub>2</sub>Si<sub>2</sub> are located at low-symmetry sites, so that the fields do not cancel; they reside above and below the centres of the uranium plaquettes. Microscopically, wavevector selection is most probably due to details of the Fermi surface; however, we can obtain a good idea of the likely modulation  $Q$  vector from the isotropic nature of the field distribution at the

silicon sites. For example, in the commensurate case  $Q = (1/2, 1/2, 1)$ , the fields on the silicon sites are only along the  $c$  axis and thus the field distribution would be highly anisotropic. Consider a wavevector  $(q, q, 1)$  (see Fig. 1). In this case, the currents are modulated within a plane with a wavelength  $2\pi/q$ , but staggered between planes. This then produces a circulating field distribution where the component of the field parallel to the  $(0, 0, 1)$  planes becomes larger and larger as  $q$  is reduced. To obtain an isotropic field distribution,  $q$  needs to be reduced to a point where the horizontal and vertical components of the field are comparable. A detailed calculation based on the above model shows that the condition of perfect isotropy yields a circle of wavevectors (Fig. 2) centred around  $Q = (0, 0, 1)$  with a radius  $q \approx 0.22$ . Relaxation of this constraint results in an annulus of possible  $Q$  vectors, as shown in Fig. 2.

Our proposal of incommensurate current ordering in URu<sub>2</sub>Si<sub>2</sub> can be tested by experiment. In particular we can Fourier-transform the real-space magnetic fields to calculate the neutron-scattering cross-section:

$$\frac{d\sigma}{d\Omega} = \left( \frac{g_N e}{8\pi\hbar c} \right)^2 |\mathbf{B}(q)|^2 = r_0^2 S(q) \quad (4)$$

Here  $|\mathbf{B}(q)|^2$  is the structure factor of the magnetic fields produced by the orbital currents and  $S(q) = |\mathbf{B}(q)|^2/(4\pi\mu_B)^2$  is the structure factor of the orbital magnetic moments, measured in units of electron Bohr magnetons ( $\mu_B$ ). The factor  $r_0 = g_N e^2/4m_e c^2$ ,  $m_e$  is the electron mass and  $g_N$  is the neutron gyromagnetic ratio. Using the vector potential from equation (3), we have calculated the magnetic field distribution for the incommensurate orbital antiferromagnet described above, and find that its Fourier transform is given by:

$$\mathbf{B}(q) = \frac{4\pi}{c} N I a^2 \sum_{\mathbf{G}_{n_1, n_2, n_3}} \delta_{q, \mathbf{Q} + \mathbf{G}} j_0 \left[ \frac{q_x a}{2} \right] j_0 \left[ \frac{q_y a}{2} \right] (1 + (-1)^{(n_1 + n_2 + n_3)}) \times \left( \left( \frac{q_y \hat{x} - q_x \hat{y}}{2q} \right) \times \hat{q} \right) \quad (5)$$

where  $j_0(x) = (\sin x)/x$ . From this expression, we can determine the intensities and the form factors associated with the diffraction. We find that there exists a set of dominant peaks associated with a constant anisotropy locus of wavevectors (Fig. 2) in the first Brillouin zone where  $S(q) = 0.18 (N I a^2/c\mu_B)$ , indicating that roughly a fifth of the total integrated weight of  $S(q)$  lies here. Using the sum rule that relates the total integrated weight to the square of the moment, and the fact that at ambient pressure only a tenth of the sample is (spin) magnetic, we find that the scattering peaks due to orbital ordering in the first Brillouin zone should have 1/50 the intensity of the analogous spin magnetic peaks at ambient pressure. We have also calculated that these peaks will have a form factor (see Fig. 2) that scales with wavevector as  $q^{-4}$ , where this power-law decay indicates an extended scattering source.

We end with remarks about the microscopic formation of these charge currents. At low temperatures, heavy electron materials form almost incompressible Fermi liquids. The large Coulomb repulsion between the Landau quasiparticles strongly suppresses on-site charge fluctuations, demanding nodes in the particle-hole wavefunction. The resulting anisotropically paired states are also favoured by the residual antiferromagnetic interactions that persist in the heavy electron fluid. Indeed, we believe that the same d-wave pairing that drives the superconducting transition in URu<sub>2</sub>Si<sub>2</sub> at  $T = 1.5$  K also plays an important role in the formation of the orbital antiferromagnetism. We have found that the development of such anisotropic charge-density wave pairing occurs naturally in a simple model of URu<sub>2</sub>Si<sub>2</sub> with nearest-neighbour antiferromagnetic

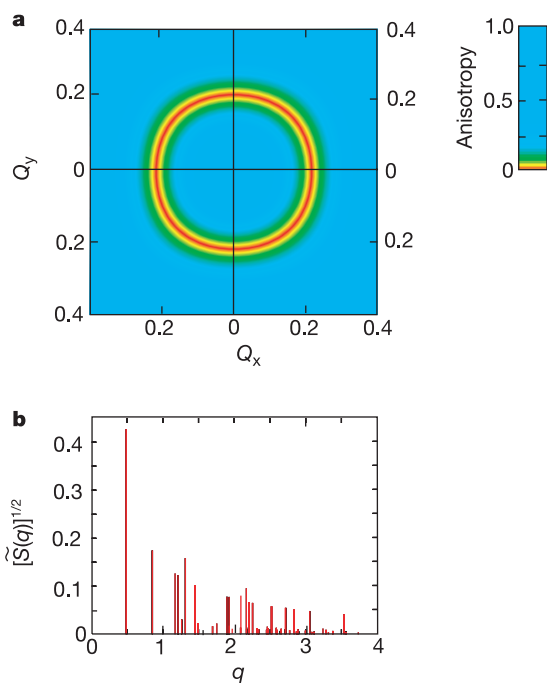


**Figure 2** An isotropic magnetic field distribution at the silicon sites can be produced by many different wave vectors  $Q$  for orbital order, all of which give qualitatively similar neutron scattering patterns. **a**, Contour plot showing locus of constant anisotropy around a ring of radius  $Q_{\perp} = 0.22$  in the vicinity of  $Q = (0, 0, 1)$ . **b**, Predicted elastic neutron scattering intensity, where  $\tilde{S}(q)^2 = S(q)^2 / (\frac{N\mu_B^2}{C_{mag}}) \approx \sqrt{|B(q)|^2}$  gives a measure of the Fourier spectrum of magnetic fields  $B(q)$ , plotted for the representative case  $Q = (0.16, 0.16, 1)$ .

interactions:

$$H_I = \sum_{\mathbf{q}} J(\mathbf{q}) \mathbf{S}(\mathbf{q}) \cdot \mathbf{S}(-\mathbf{q}) \quad (6)$$

Here  $\mathbf{S}(\mathbf{q})$  is the Fourier transform of the magnetization at wavevector  $\mathbf{q}$  and  $J(\mathbf{q}) = 2J(\cos q_x + \cos q_y)$  for a nearest-neighbour interaction between adjacent U atoms in the basal plane. Expanding this interaction in terms of quasiparticle operators, we find that it can be rewritten as a sum of attractive interactions in four independent anisotropic charge-density wave channels:

$$H_I = -J \sum_{\Gamma=1,4} (\gamma_{k_1}^{\Gamma})^* \gamma_{k_2}^{\Gamma} \rho_{k_1}(Q) \rho_{k_2}(-Q) \quad (7)$$

Here  $\rho_{\mathbf{k}}(Q) = \sum_{\sigma=\pm 1/2} c_{k-Q/2\sigma}^{\dagger} c_{k+Q/2\sigma}$  is the charge-density operator at wavevector  $Q$ , expressed in terms of creation and annihilation operators of the heavy quasiparticles. The form factors are  $\gamma^{1,2}(\mathbf{k}) = \cos(k_x) \pm \cos(k_y)$ ,  $\gamma^{3,4}(\mathbf{k}) = i(\sin(k_x) \pm \sin(k_y))$ . Of these four possibilities, channels 1 and 3 do not have nodes, and are therefore suppressed by local Coulomb interactions. In the remaining two channels, only  $\Gamma = 4$  breaks time reversal symmetry, giving rise to incommensurate orbital currents. One of the questions for further study concerns the excitations of this mean-field state. URu<sub>2</sub>Si<sub>2</sub> is known to develop a dispersing singlet excitation<sup>10</sup> at  $T = T_0$ . This mode was previously attributed to spin antiferromagnetism, now known to be absent from the hidden order phase<sup>17</sup>. We plan to study the possible identification of this propagating mode with the gapless phason associated with the uniform translation of an incommensurate orbital antiferromagnet.

Thus we have discussed the theoretical implications of two recent NMR experiments on the hidden order in URu<sub>2</sub>Si<sub>2</sub>. Pressure-dependent measurements indicate that it is completely independent of the spin magnetism in this material. We argue that the develop-

ment of isotropically distributed magnetic fields at the silicon sites at  $T = T_0$  implies that the hidden-order parameter breaks time-reversal symmetry. The size and the isotropy of these observed local fields lead us to propose that URu<sub>2</sub>Si<sub>2</sub> becomes an incommensurate orbital antiferromagnet at  $T < T_0$ . The heavy electron mass reduces the saturation value of the orbital moment, accounting for the sizable entropy loss at the transition and the scale of the associated critical field. We calculate the positions, intensities and form factor associated with the resulting neutron-scattering peaks so that this proposal can be tested by experiment. □

Received 30 January; accepted 29 April 2002; doi:10.1038/nature00795.

- Goodstein, D. L. *States of Matter* (Dover, New York, 1985).
- Buyers, W. J. L. Low moments in heavy-fermion systems. *Physica B* **223** & **224**, 9–14 (1996).
- Miyake, K., Schmitt-Rink, S. & Varma, C. M. Spin-fluctuation-mediated even-parity pairing in heavy fermion superconductors. *Phys. Rev. B* **34**, 6554–6556 (1986).
- Palstra, T. T. M. *et al.* Superconducting and magnetic transitions in the heavy fermion system URu<sub>2</sub>Si<sub>2</sub>. *Phys. Rev. Lett.* **55**, 2727–2730 (1985).
- Miyako, Y. *et al.* Magnetic properties of U(Ru<sub>1-x</sub>Rh<sub>x</sub>)<sub>2</sub>Si<sub>2</sub> single crystals ( $0 < x < 1$ ). *J. Appl. Phys.* **70**, 5791–5793 (1991).
- Ramirez, A. P. *et al.* Nonlinear susceptibility as a probe of tensor spin order in URu<sub>2</sub>Si<sub>2</sub>. *Phys. Rev. Lett.* **68**, 2680–2683 (1992).
- De Visser, A. *et al.* Thermal expansion and specific heat of monocrystalline URu<sub>2</sub>Si<sub>2</sub>. *Phys. Rev. B* **34**, 8168–8171 (1986).
- Palstra, T. T. M., Menovsky, A. A. & Mydosh, J. A. Anisotropic electrical resistivity of the magnetic heavy-fermion superconductor URu<sub>2</sub>Si<sub>2</sub>. *Phys. Rev. B* **33**, 6527–6530 (1986).
- Mason, T. E. & Buyers, W. J. L. Spin excitations and the electronic specific heat of URu<sub>2</sub>Si<sub>2</sub>. *Phys. Rev. B* **43**, 11471–11473 (1991).
- Broholm, C. *et al.* Magnetic excitations in the heavy-fermion superconductor URu<sub>2</sub>Si<sub>2</sub>. *Phys. Rev. B* **43**, 12809–12822 (1991).
- Mentink, S. A. M. *et al.* Gap formation and magnetic ordering in URu<sub>2</sub>Si<sub>2</sub> probed by high-field magnetoresistance. *Phys. Rev. B* **53**, R6014–R6017 (1996).
- van Dijk, N. H. *et al.* Specific heat of heavy-fermion URu<sub>2</sub>Si<sub>2</sub> in high magnetic fields. *Phys. Rev. B* **56**, 14493–14498 (1997).
- Mason, T. E. *et al.* Nontrivial magnetic order in URu<sub>2</sub>Si<sub>2</sub>? *J. Phys. Condens. Mat.* **7**, 5089–5096 (1995).
- Amitsuka, H. *et al.* Effect of pressure on tiny antiferromagnetic moment in the heavy-electron compound URu<sub>2</sub>Si<sub>2</sub>. *Phys. Rev. Lett.* **83**, 5114–5117 (1999).
- Fisher, R. A. *et al.* Specific heat of URu<sub>2</sub>Si<sub>2</sub>: Effect of pressure and magnetic field on the magnetic and superconducting transitions. *Physica B* **163**, 419–423 (1990).
- Shah, N., Chandra, P., Coleman, P. & Mydosh, J. A. Hidden order in URu<sub>2</sub>Si<sub>2</sub>. *Phys. Rev. B* **61**, 564–569 (2000).
- Matsuda, K. *et al.* Spatially inhomogeneous development of antiferromagnetism in URu<sub>2</sub>Si<sub>2</sub>: Evidence from <sup>29</sup>Si NMR under pressure. *Phys. Rev. Lett.* **87**, 087203-1–087203-4 (2001).
- Luke, G. M. *et al.* Muon spin relaxation in heavy fermion systems. *Hyper. Inter.* **85**, 397–409 (1994).
- Chandra, P., Coleman, P. & Mydosh, J. A. Pressure-induced magnetism and hidden order in URu<sub>2</sub>Si<sub>2</sub>. Preprint cond-mat/0110048 at (<http://xxx.lanl.gov>) (2001).
- Bernal, O. O. *et al.* <sup>29</sup>Si NMR and hidden order in URu<sub>2</sub>Si<sub>2</sub>. *Phys. Rev. Lett.* **87**, 153–156 (2001).
- Schlichter, C. P. *Principles of Magnetic Resonance* (Springer, Berlin, 1978).
- Halperin, B. I. & Rice, T. M. in *Solid State Physics* (eds Seitz, F., Turnbull, D. & Ehrenreich, H.) Vol. 21, 116–192 (Academic, New York, 1968).
- Affleck, I. & Marston, J. B. Large- $n$  limit of the Heisenberg-Hubbard model: Implications for high  $T_c$  superconductors. *Phys. Rev. B* **37**, 3774–3777 (1988).
- Kotliar, G. Resonating valence bonds and D-wave superconductivity. *Phys. Rev. B* **37**, 3664–3666 (1988).
- Nersisyan, A. A. & Vachnadze, G. E. Low-temperature thermodynamics of two-dimensional orbital antiferromagnet. *J. Low-Temp. Phys.* **77**, 293–303 (1989).
- Schulz, H. J. Fermi surface instabilities of a generalized two-dimensional Hubbard model. *Phys. Rev. B* **39**, 2940–2943 (1989).
- Hsu, T. C., Marston, J. B. & Affleck, I. Two observable features of the staggered-flux phase at nonzero doping. *Phys. Rev. B* **43**, 2866–2877 (1991).
- Lee, P. A. Orbital currents in underdoped cuprates. Preprint cond-mat/0201052 at (<http://xxx.lanl.gov>) (2002).
- Chakravarty, S., Laughlin, R. B., Morr, D. K. & Nayak, C. Hidden order in the cuprates. *Phys. Rev. B* **63**, 094503-1–094503-10 (2001).
- Kee, H.-Y. & Kim, Y. B. Specific heat anomaly in the D-density wave state and emergence of incommensurate orbital antiferromagnetism. Preprint cond-mat/0111461 at (<http://xxx.lanl.gov>) (2001).

#### Acknowledgements

We acknowledge discussions with G. Aeppli, H. Amitsuka, O. Bernal, S. Chakravarty, L.P. Gorkov, G. Lonzarich, K. McEuen, D. McLaughlin, D. Morr and C. Nayak. P. C. and V. T. are supported by the National Science Foundation.

#### Competing interests statement

The authors declare that they have no competing financial interests.

Correspondence and requests for materials should be addressed to P.C. (e-mail: coleman@physics.rutgers.edu).